Electronic Supporting Information

Simply Realizing "Water Diode" Janus Membranes for Multifunctional Smart Applications

Zhenxing Wang,‡[a] Xiaobin Yang,‡[a] Zhongjun Cheng,[b] Yuyan Liu,[a] Lu Shao,[a] and Lei Jiang[c]

[a] *MIIT Key Laboratory of Critical Materials Technology for New Energy Conversion and Storage, State Key Laboratory of Urban Water Resource and Environment, School of Chemistry and Chemical Engineering, Harbin Institute of Technology, Harbin 150001, PR China.*

[b] *Natural Science Research Center, Academy of Fundamental and Interdisciplinary Sciences, Harbin Institute of Technology, Harbin 150001, China.*

[c] *Institute of Chemistry, Chinese Academy of Sciences, Beijing 10080, Chin.*

‡ *These authors contributed equally to this work*

Contents:

1. Experimental Section

***Materials*:** PET/PTFE porous membranes were commercially available from Beijing Shenghe, China. The commercial PET/PTFE membrane is hydrophobic, the pore size is about 0.22 μm, the porosity of the membrane is about 86%, and the thickness of the membrane is about 110 μm. Dopamine hydrochloride (DA) and polyethylene glycol (M_w=1000) were obtained from Sigma-Aldrich. Tannic acid (TA), tris(hydroxymethyl)aminomethane (Tris), diethylenediamine (DETA), 11-mercaptoundecanoic acid ($HS(CH_2)_{10}COOH$), 1-decanethiol ($HS(CH_2)_9CH_3$) and silver nitrate ($AgNO_3$) were purchased from Aladdin (China). Iron (III) chloride hexahydrate ($FeCl_3$• $6H_2O$), ethylene glycol, sodium acetate (NaAc), hydrochloric acid (HCl), anhydrous ethanol, petroleum ether, dichloroethane, oil red and methylene blue were purchased from Tianjin Kermel Chemical Reagent Co., Ltd. (China). All the chemicals were used as received. Ultrapure water (18.0 MΩ•cm) was produced using a Sartorius AG Arium system and used in all experiments.

***Preparation of hydrophilic PET/PTFE membrane (PET/PTFE@TA-DETA)*:** The PET/PTFE composite membrane was pre-wetted by ethanol and then immersed in 100 mL of aqueous solution (including 0.2 g of TA and 1.2 g of DETA) for 6 h at room temperature to prepare the PET/PTFE@TA-DETA. The obtained membrane was washed with deionized water several times to remove unreacted reagent and then kept in water for the next modification.

***Preparation of Janus membranes (JM)*:** A JM with a thick hydrophilic layer and a thin hydrophobic layer was fabricated via simply peeling off the top skin of a hydrophilic PET/PTFE porous membrane (prior drying at 60 °C overnight) using adhesive tape. The surface after peeling is defined as the top surface, while the other surface is the back surface. For comparison, we also prepared a non-Janus membrane by treating the top surface of the JM with an O_2 plasma, which can transform the thin hydrophobic top surface into a

hydrophilic surface while maintaining the pore size of the membrane. The JM was treated with O_2 for 30 min with the hydrophobic side exposed to the plasma flux. The gas flow of O_2 was set at 30 sccm, and the forward RF Target power was 65 W.

***Preparation of magnetic Janus membranes (MJM)*:** Fe_3O_4 nanoparticles were prepared according to a modified literature method.[1] Briefly, $FeCl_3 \cdot 6H_2O$ (2.7 g) was dissolved in ethylene glycol (80 mL), followed by the addition of NaAc (7.2 g) and polyethylene glycol (2.0 g, M_w=1000). The mixture was stirred vigorously and then sealed in a Teflon-lined stainless steel autoclave. The autoclave was heated to, and maintained at, 200 °C for 8 h and then allowed to cool to room temperature. The black products were washed several times with ethanol and kept in ethanol with an oil seal before use. To fabricate the MJM, a hydrophilic PET/PTFE porous membrane was ultrasonically cleaned in water and then ethanol for 5 min each. Then, the membrane was immersed in an aqueous mixture (pH = 1, 200 mL) comprised of DA (2 mg mL^{-1}) and Fe_3O_4 (5 mg mL^{-1}) with shaking for 12 h. After being rinsed with water, the membrane was immersed into another aqueous solution (pH=8.5, 200 mL) including DA (2 mg mL^{-1}) and PEI (3 mg mL^{-1}) with shaking for another 12 h. The obtained membrane with multifunctional coatings was washed with water several times and then dried at 60 °C. Peeling off the top skin layer of the obtained membrane can easily transform it into a multifunctional Janus membrane with asymmetric wettability. The surface after peeling is defined as the top surface, while the other surface is the back surface.

***Preparation of pH-responsive Janus membranes (pH-rJM)*:** A hydrophilic PET/PTFE porous membrane was immersed in a DA aqueous solution (pH=8.5, 2 mg mL^{-1}, 200 mL) with shaking for 12 h. After being rinsed with water, the membrane was then immersed into $AgNO_3$ aqueous solution (100 mL, 1 mg mL^{-1}) with shaking for 24 h. After being washed with water and ethanol several times, the obtained membrane was immersed into an ethanol solution (100 mL) containing $HS(CH_2)_9CH_3$ (1.2 mM) and $HS(CH_2)_{10}COOH$ (0.8 mM) for 24

h to form pH-responsive coatings. Afterwards, the membrane was washed thoroughly with ethanol and heated in a vacuum oven for 6 h at 50 °C. Peeling off the top skin layer produced the pH-responsive Janus membrane (pH-rJM). The surface after peeling is defined as the top surface, while the other surface is the back surface. The flat pH-responsive Ag surface was prepared by simply immersing the flat Ag substrate into the ethanol solution with the same thiol molecules.

***Characterizations*:** XPS analysis was carried out on a Shimadzu AXIS Ultra DLD spectrometer using an Al-Kα X-ray source. All core-level spectra were obtained at a photoelectron take-off angle of 90° with respect to the sample surface. Scanning electron microscopy (SEM) images were acquired using a Hitachi S-4500. The water contact angles were measured by a contact angle measuring system (SL 200KB, China). The droplet size of the oil droplets in an emulsion were observed using optical microscopy (BM-60XCC). UV– Vis spectra were recorded using a Shimadzu UV2501 spectrophotometer.

***Unidirectional permeation, water droplet collection, and critical hydrostatic pressure*:** For unidirectional permeation experiments, the hydrophilic side of JM was pre-wetted by water. Then, the hydrophobic side of JM was wetted by petroleum ether. Afterwards, the JM was fixed at the water and oil (petroleum ether) interface, and a water droplet (approximately 200 μL) was dropped on the surface of the Janus membrane to evaluate the unidirectional permeation property. For collection of water droplets, a mini Janus boat was prepared by folding the JM or MJM (the hydrophilic surface act as the outer surface of the boat), and the hydrophilic side was pre-wetted by water. Then, the collector was placed on the oil surface to trap the water droplets (dyed by rose bengal) dispersed in the oil solution.

Hydrostatic pressure (HP) was measured in order to characterize the pressure that would allow water to break through the JM. The thick hydrophilic layer of JM was wetted by water, and the thin hydrophobic layer was wetted by oil (dichloroethane). The JM was then fixed on

a transparent tube with the thick hydrophilic layer oriented upward. Water was then gradually added into the tube. After each small addition, the water-filled tube was held for at least 1 min to determine whether the water penetrated through the JM. The height of the water column was recorded as the critical hydrostatic pressure. For comparison, the HP of the corresponding homogeneous hydrophilic membrane was also measured using the same method.

2. Additional data and figures

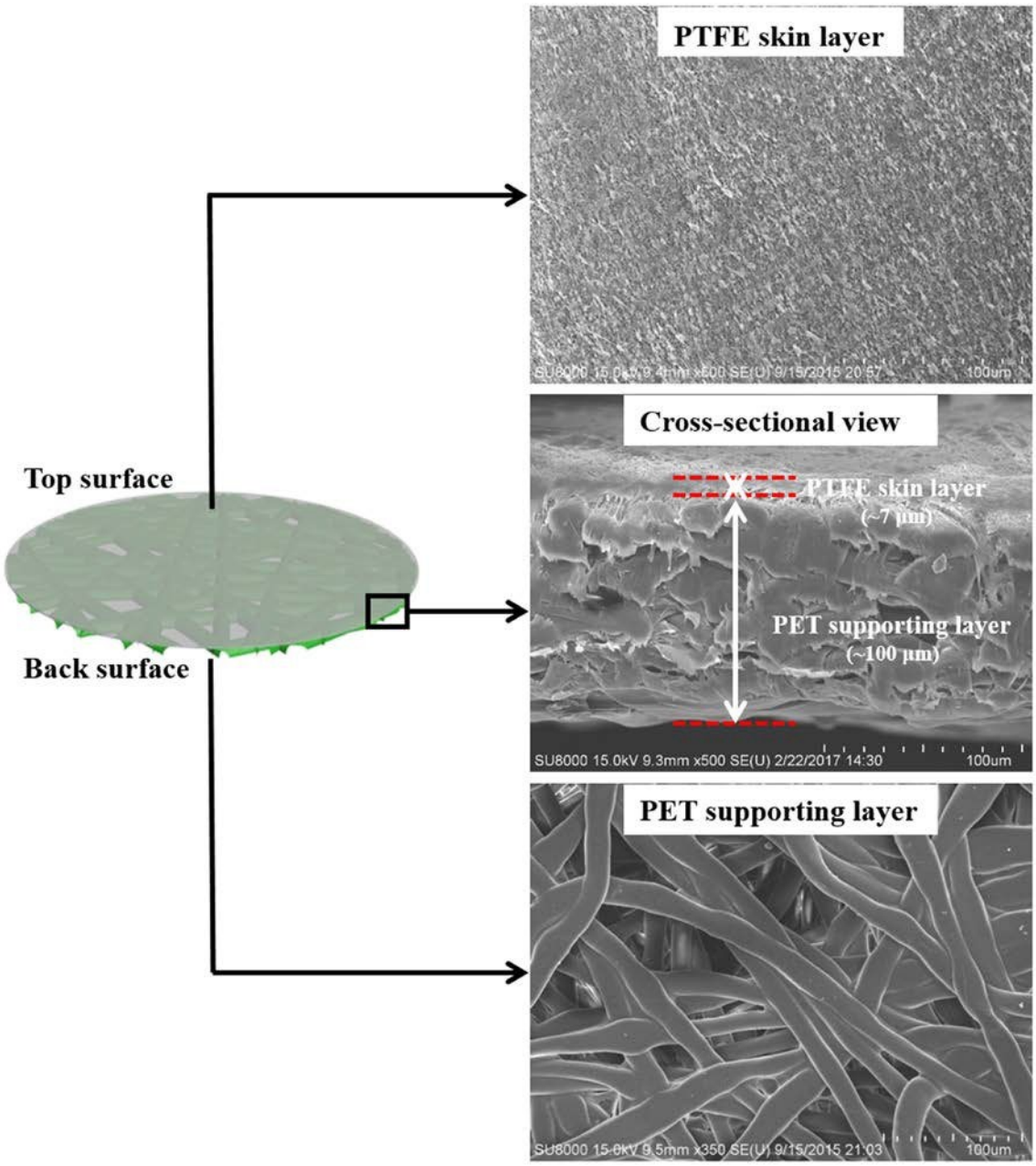

Fig. S1 Schematic illustration of the composite structure of the PET/PTFE membrane and the SEM images of the two surfaces and the cross-sectional location. The top surface is referred to the PTFE skin layer, and the back surface is the PET supporting layer.

As shown in Fig. S1. The PTFE skin layer of the PET/PTFE membrane is relatively thin (ca. 7 μm) and the PET supporting layer is relatively thick (ca. 100 μm). The cross-sectioal view was obtained from the specimen prepared by the scissor instead of the liquid nitrogen

assisted fracture because the PET/PTFE membrane cannot be fractured by immersing in the liquid nitrogen. Thus, the PET fiber located in the supporting layer seems to be bonded with each other. When the PTFE skin layer was peelled off from the modified hdrophilic membrane by the adhesive tap, the resultant exposed top surface is hydrophobic and the hydrophobic layer is very thin *versus* the modified hydrophilic PET supporting layer.

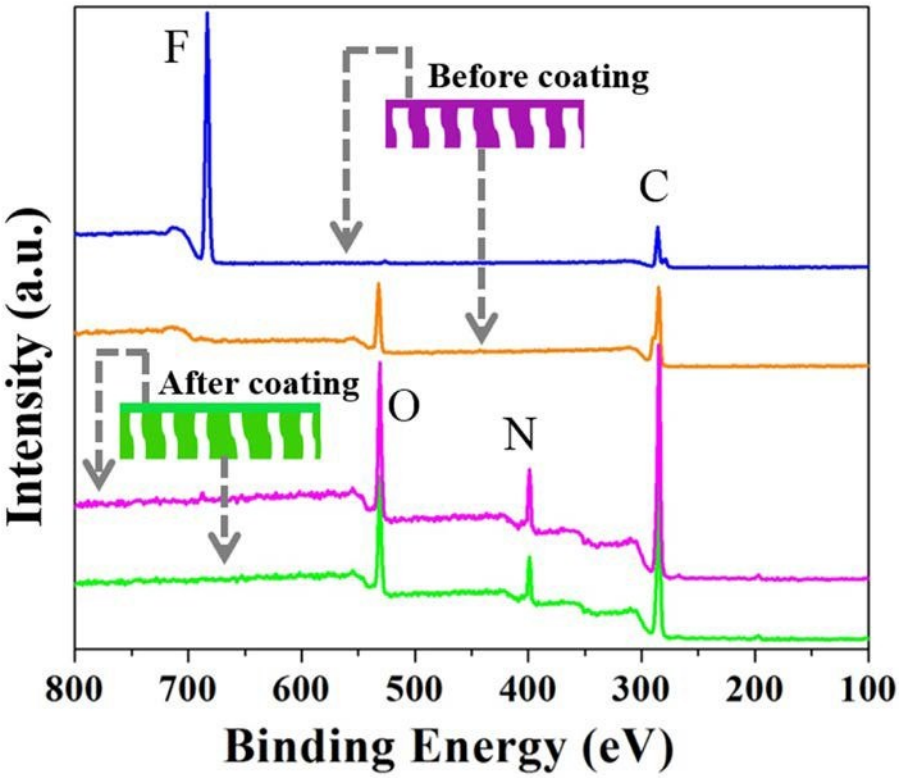

Fig. S2 XPS spectra of the top and back surface of the PET/PTFE membrane before and after TA-DETA coating (PET/PTFE@TA-DETA), respectively.

As shown in Fig. S2, the formation of TA-DETA coatings could be confirmed by the new N feature on both modified sides. Besides, the disappeared F element on the modified top surface and the increased O element on the back surface further demonstrate the formation of TA-DETA coatings.

Table S1 The elemental compositions of the top and back surfaces of the PET/PTFE and PET/PTFE@TA-DETA, respectively.

Top surface	Composition (At.%)			
	C	O	F	N
PET/PTFE (top surface)	56.2	/	43.8	/
PET/PTFE@TA-DETA (top surface)	53.6	33.8	/	12.6
PET/PTFE (back surface)	70.4	29.6	/	/
PET/PTFE@TA-DETA (back surface)	57.3	30.8	/	11.9

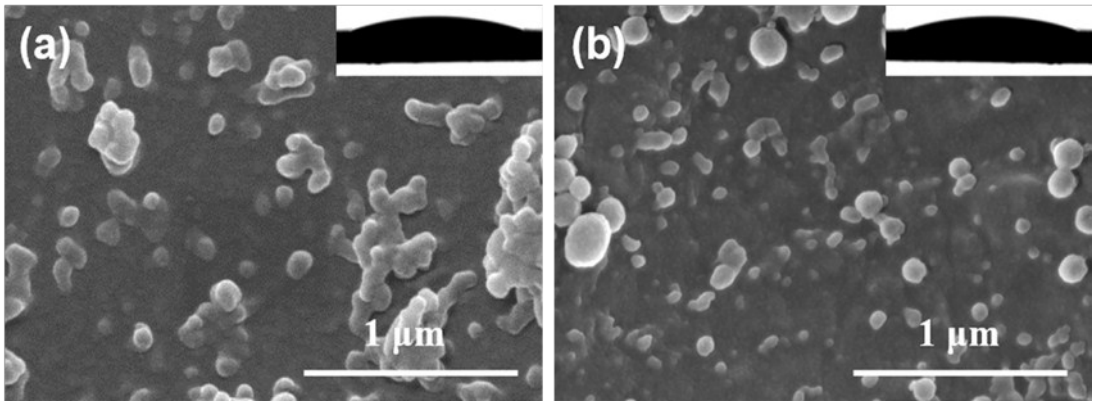

Fig. S3. SEM images of the back surface on the PET/PTFE@TA-DETA membrane before and after rinsing for about 3 h, insets are the shapes of a water droplet on the membrane.

From the two figures, it can be seen that the morphology and wettability have no apparent variation after rinsing, demonstrating good stability of the TA-DETA coating on the PET/PTFE substrate. Herein, we just investigated the back surface because the top PTEF layer was peeled off for the fabrication of JM membrane.

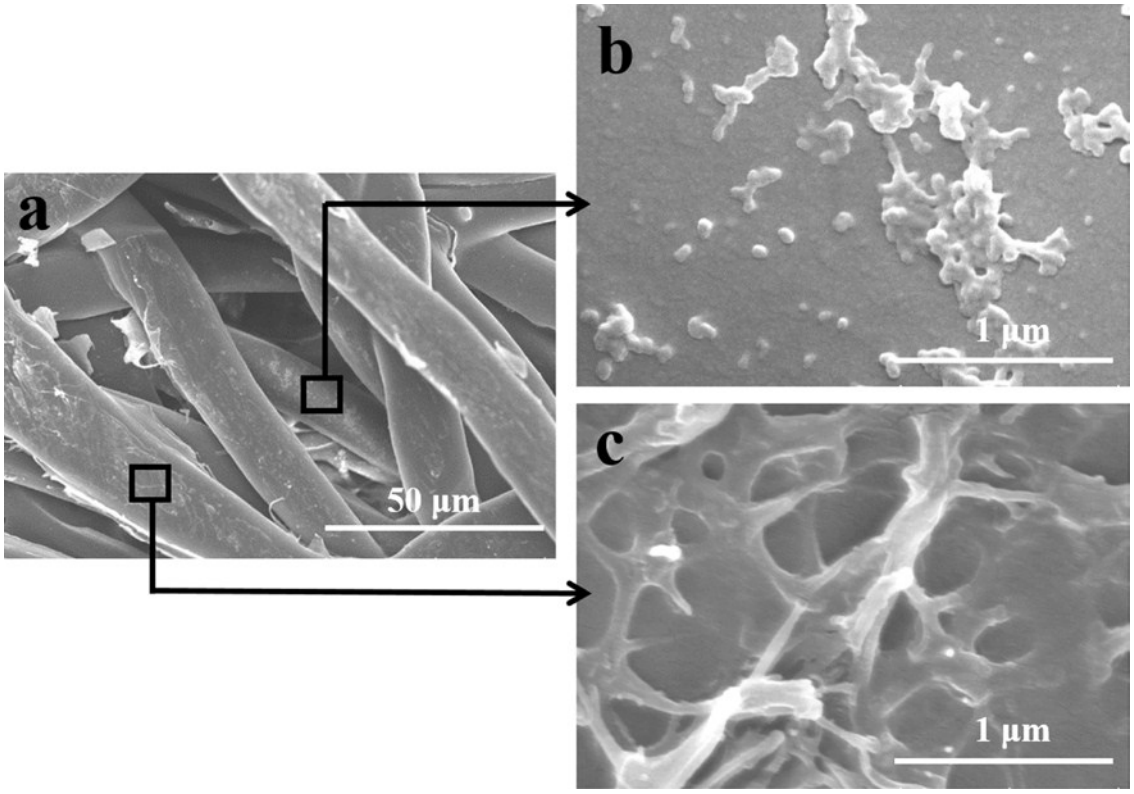

Fig. S4 a) SEM image of two kinds of rough structures observed on different position of the top surface of JM. b) SEM image of the inner PET fiber surface. c) SEM image of the topmost PET fiber surface.

As shown in Fig. S4, on the inner PET fiber surface, there was a layer of coating ascribed to TA/DETA with scattered dots, and on the topmost PET fiber surface there were some residual tearing PTFE fragments after the peeling process.

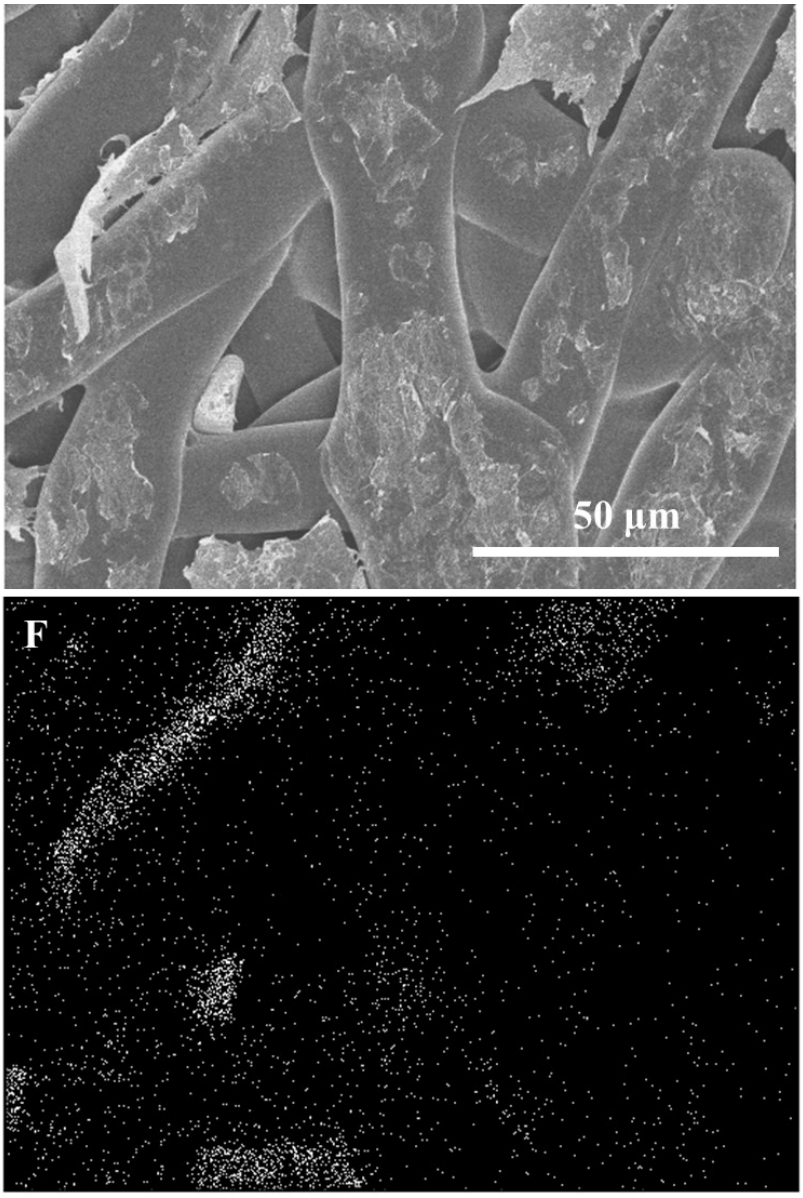

Fig. S5. EDX mapping of F element on the top surface of the JM (PET@TA-DETA).

From the EDX mapping shown in Fig. S5, abundant F element dots are scattered on the top surface of the JM. Meanwhile, the distributed density of F element dots is consistent with the size and scale of the located fragments. This result confirmed that the adhesive tap teared the skin layer and exposed the hydrophobic nature of the PTFE material. Moreover, with the aid of exposed unmodified surface of the PET fiber, the resultant membrane received a new-born hydrophobic top surface.

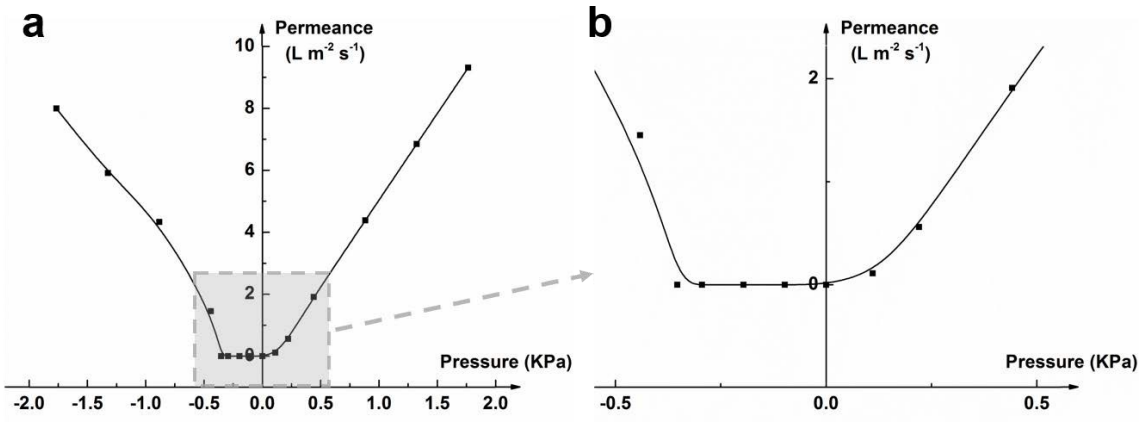

Fig. S6 The permeability of JM in both directions as a function of pressure. Figure b is the magnified image of gray region of figure a. The positive direction of X axis represents that the hydrophobic surface is put upwardly, the negative direction represents that the hydrophilic surface is put upwardly.

It can be seen that when the hydrophobic layer is put upwardly, the permeation can be happened under a very small pressure, and the flux is increased as the pressure is increased. When the hydrophilic surface is put upwardly, the permeation can happen only when the pressure is larger than a certain value (about 0.35 KPa), and the flux would be increased as the pressure is further increased. These results further confirm that the JM has the asymmetric wettability and can act as a "water diode".

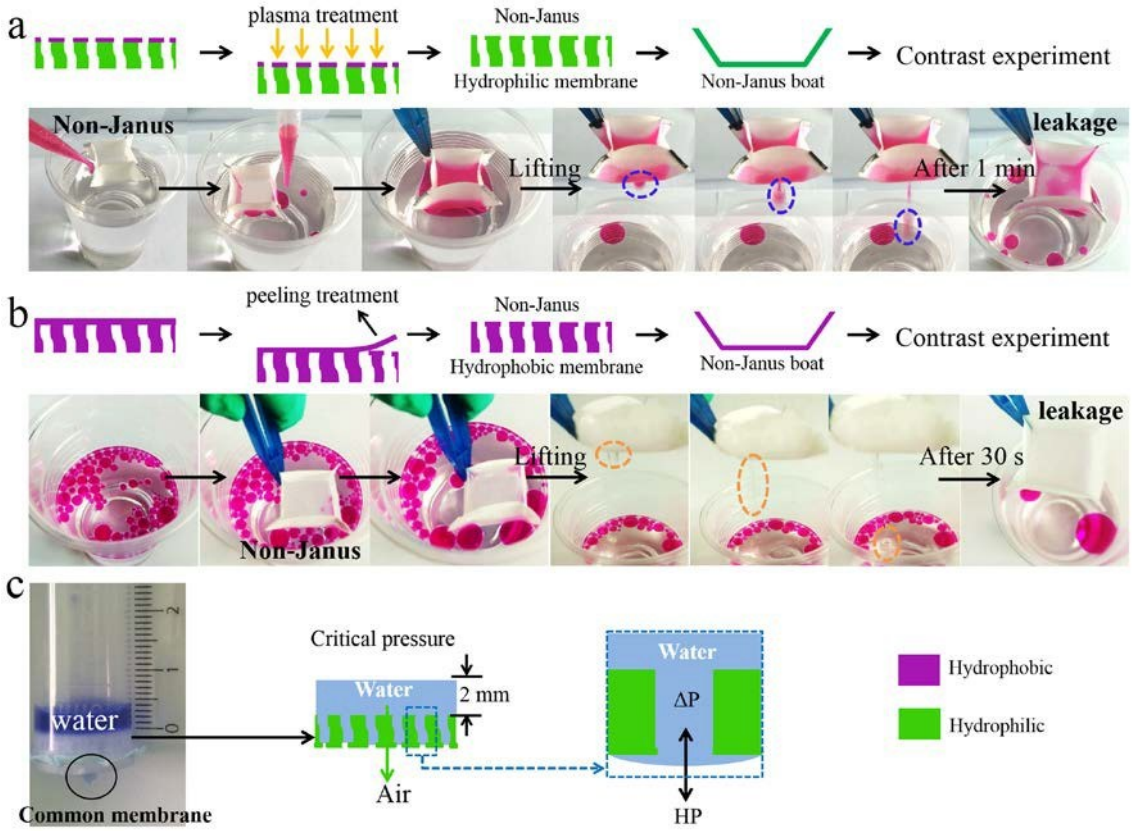

Fig. S7. a) Schematic illustration and photo images showing the leakage of water from a non-Janus hydrophilic boat (the water droplets floating on oil surface were dyed with rhodamine B, and the colorless oil is dichloroethane). b) Schematic illustration and photo images showing the leakage of oil from a non-Janus hydrophobic boat. c) Optical image and schematic illustration of the critical pressure for non-Janus hydrophilic membrane.

The non-Janus hydrophilic boat was prepared by folding the JM membrane, on which the top hydrophobic surface has been treated by plasma. The non-Janus hydrophilic boat could realize water collection, however, once lifting boat into the air, the leakage of collected water was inevitable, similar to "drawing water with a sieve" (Fig. S7a). Similarly, a non-Janus hydrophobic boat was also prepared by peeling off the skin layer of the pristine hydrophobic PET/PTFE membrane (Fig. S7b). When the non-Janus hydrophobic boat contacted the oil-water mixture, it could only collect oil and could not collect water because of its hydrophobic feature. However, even so, the collected oil would also leak out when the boat was lifted into

the air. These two contrast tests confirmed the lossless transportation property of the Janus boat was due to the asymmetric wettability. To explain the water lossless transportation of the JM based boat, the breakthrough pressures of JM and derived non-Janus hydrophilic membrane were measured for contrast. For the non-Janus hydrophilic membrane, the Laplace pressure can be represented by $\Delta P = 0$, resulting the very low breakthrough pressure (only approximately 2 mm H_2O, Fig. S7c).

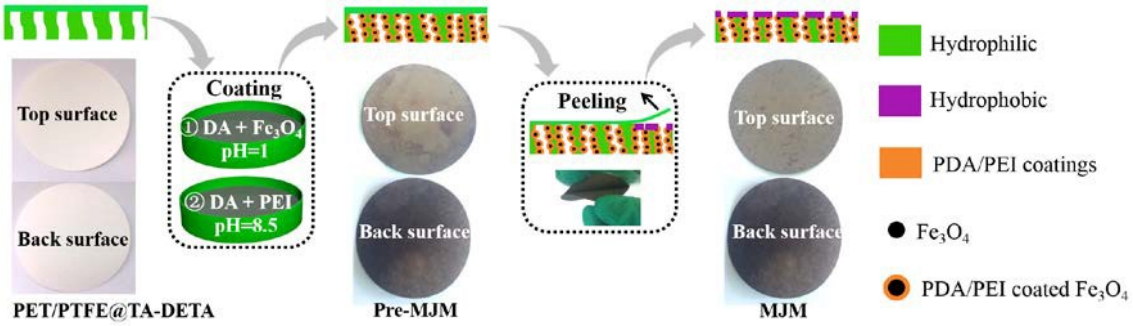

Scheme S1 Schematic and photographs showing the preparation of magnetic JM (MJM) *via* the coating and peeling strategy.

a)

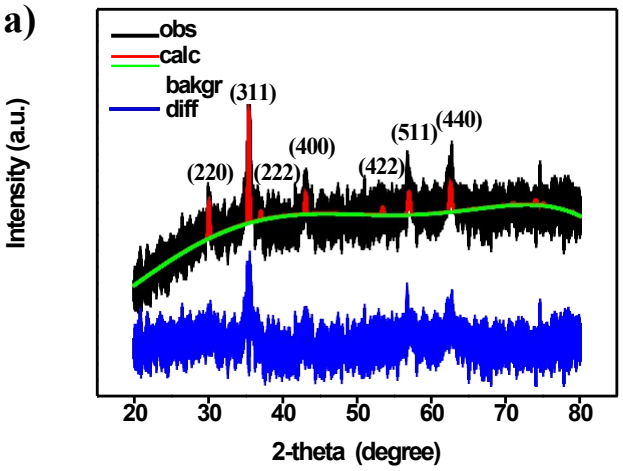

b)

Lattice parameter of Fe_3O_4 calculated by Rietveld refinement

a = b = c (Å)	**8.386192**
R_p (%)	**3.44**
R_{wp} (%)	**2.67**
χ^2	**1.481**

Fig. S8 XRD results of the synthetic Fe_3O_4: a) Rietveld refinement of profile; b) Lattice parameter results.

As shown in Fig. S8a, from the XRD pattern of the synthetic powder (black line is the experimental result), the characteristic 2θ peaks centered at 30.1°, 35.5°, 37.1°, 43.1°, 53.4°, 57.0°, and 62.6° are corresponding to (220), (311), (222), (400), (422), (511), and (440) facets, respectively, well according with the standard pattern of magnetite from the JCPDS card (File no.19-0629). Moreover, the obtained XRD profile was also analyzed by the Rietveld refinement with GSAS-EXPGUI software.[2] During the refinement, Fd-3m space group was employed as the initial model, then lattice parameter, peak shape, background and Uiso parameter were refined. Fig. S8a shows the experimental and calculated XRD profiles of the Fe_3O_4. The calculated Lattice parameters are listed in Fig. S8b, the small value of χ^2, R_{wp} and R_p indicate the good agreement between the observed and calculated data.

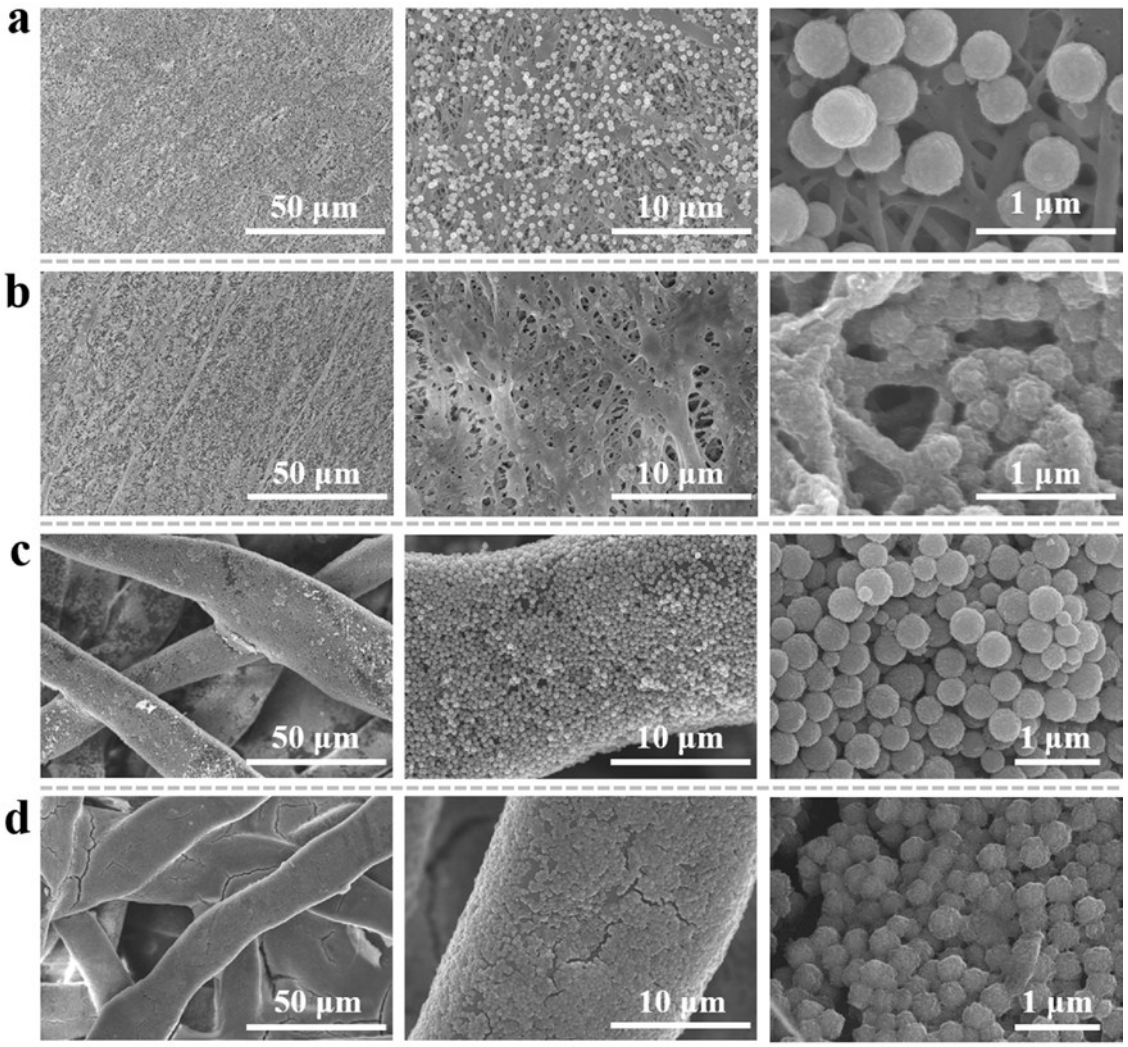

Fig. S9 SEM images with different magnification of the top surfaces of membrane a) after DA/Fe_3O_4 coating and b) follow-up PDA/PEI coating, respectively. and c, d) the corresponding back surfaces.

From SEM images of the both sides of the modified membranes, the surface maintained the porous structures of the membrane. After DA/Fe_3O_4 coating, Fe_3O_4 nanoparticles were incorporated on the membrane (Fig. S9a, S9c). After PDA-PEI coating, the surfaces of the resultant Fe_3O_4 nanoparticles (Fig. S9b, S9d) become more rugged when compared with the relatively smooth surface of the pristine Fe_3O_4 nanoparticles.

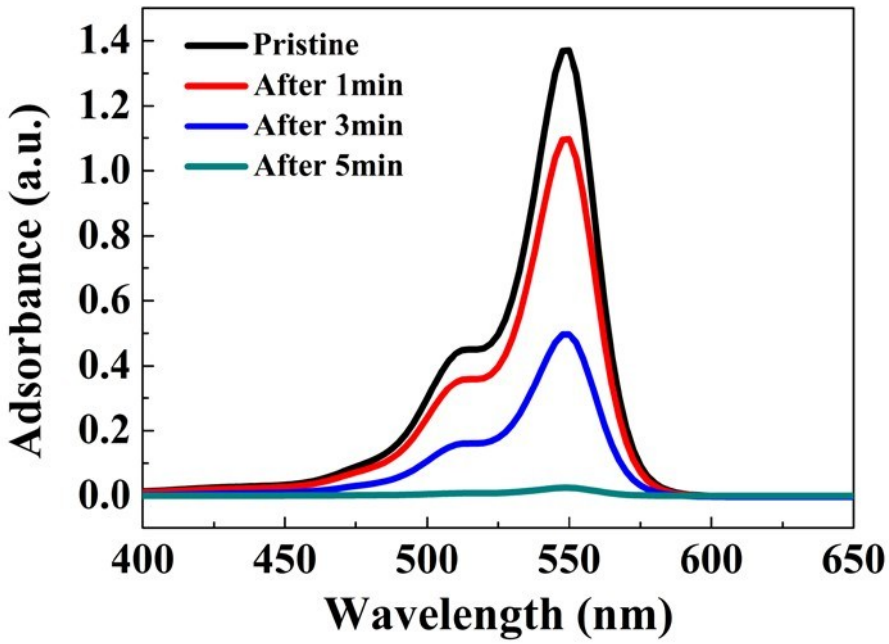

Fig. S10 The UV-Vis spectra of the collected RB solution in MJM folded boat for different duration.

From the displayed UV-Vis spectra of the collected RB solution in MJM folded boat for different duration, the adsorption of RB dye about MJM toward the collected RB solution is obviously effective and efficient. There is a large adsorbance intensity decline and nealy no charateristic peaks of RB after the in situ decontamination of the collected wastewater within 5 min. This data is used for confirmation of the integration of both magnetism and adsorptive ability of the MJM.

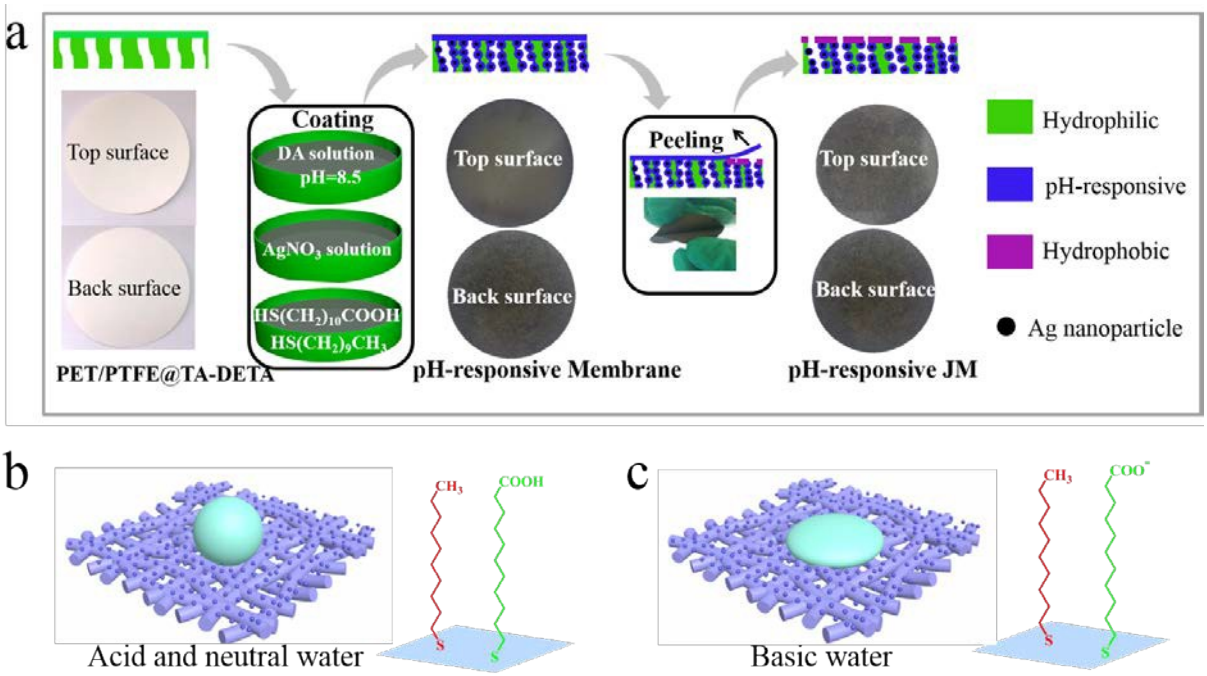

Scheme S2. (a) Schematic and photograph showing the preparation of pH-responsive Janus membrane (pH-rJM) *via* the coating and peeling strategy. Schematic illustration of the shapes of the water droplets on the surface (b) for acid and neutral water, the carboxylic acid groups are protonated, the surface is hydrophobic; (c) for basic water, the carboxylic acid groups are deprotonated, the surface is hydrophilic.

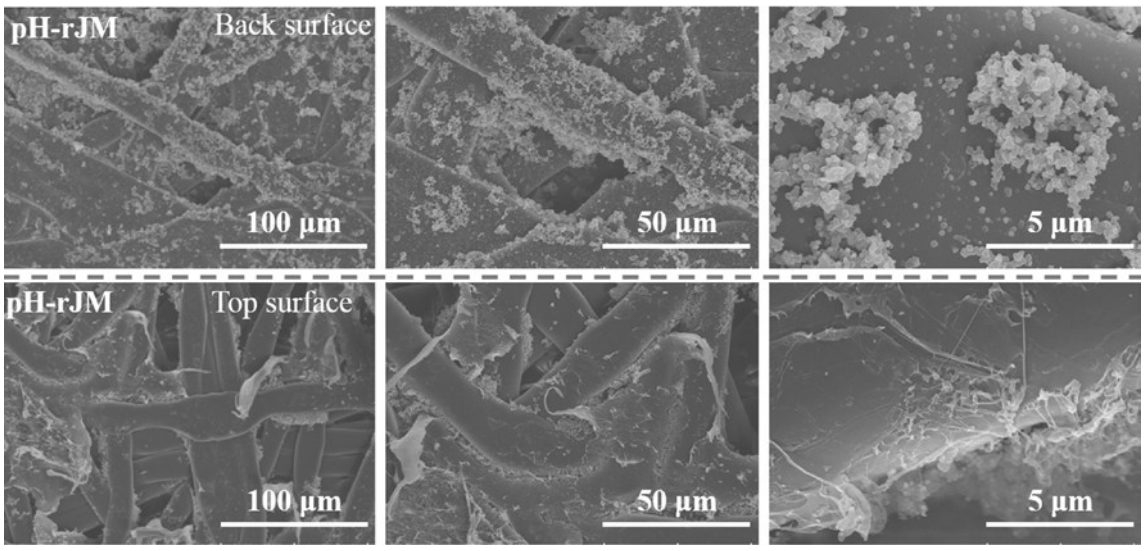

Fig. S11 SEM images of the back and top surface of the pH-rJM.

Fig. S11 presents the SEM images of pH-rJM, a large amount of nanoparticles are scatterted on the back surfaces and the inner fiber surfaces of the top surfces. About the top surfaces, there are the charateristic tearing PTFE fragements and exposed unmodified PET fiber surfaces.

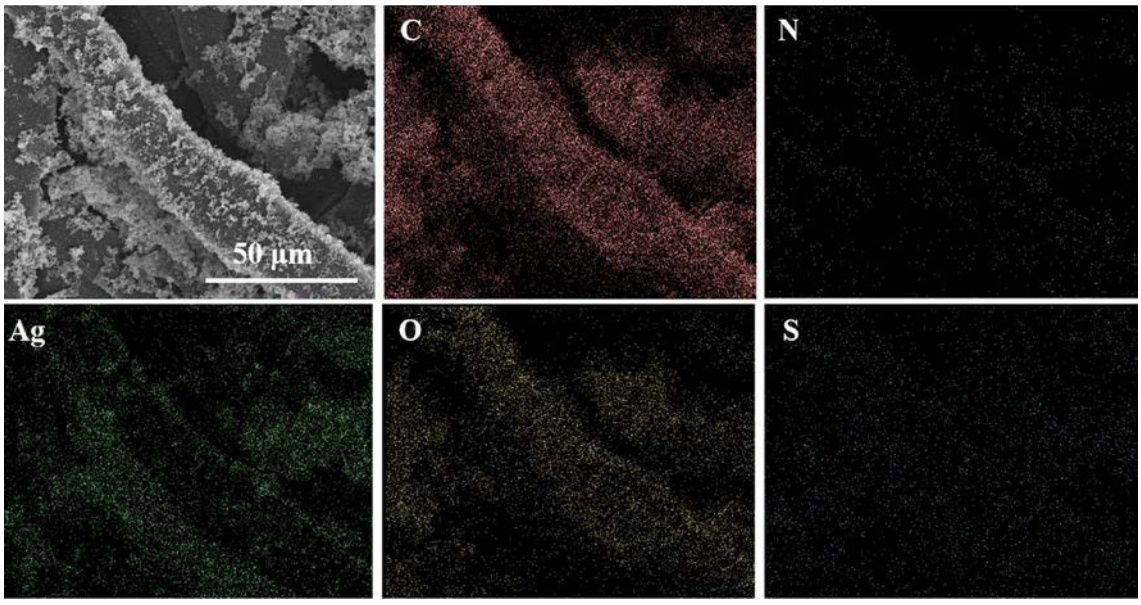

Fig. S12 EDX mapping of the back surface of the pH-rJM.

As shown in Fig. S12, the back surface of the pH-rJM is fairly rough. From the EDX mapping, a large amount of N, Ag, S dots distributed on the scanning region. N element was derived from TA/DETA and PDA coating, Ag element from Ag nanoparticle, S element from the mixed mercaptan modification. These characteristic element distribution confirmed the success of every single modification step.

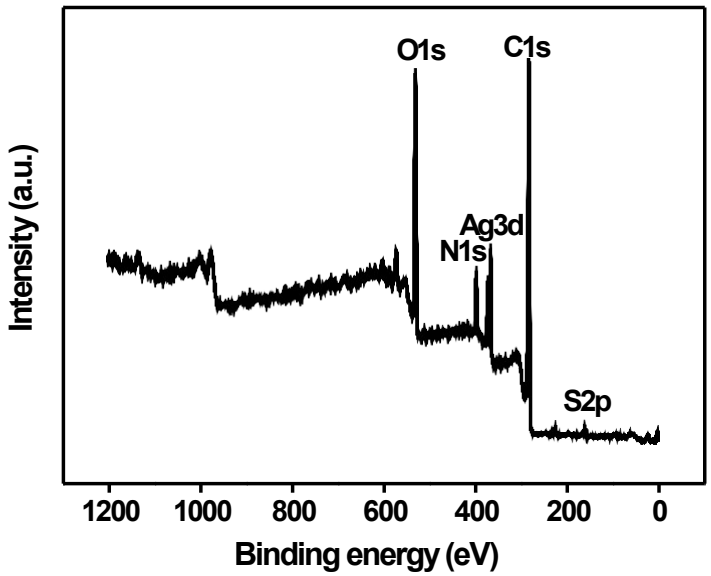

Fig. S13 XPS survey spectrum of the back surface of the pH-responsive membrane.

It can be seen that elements C, O, N, Ag, and S can be observed, the presence of S inditactes that the thiol molecules have been assembled onto the substrate.

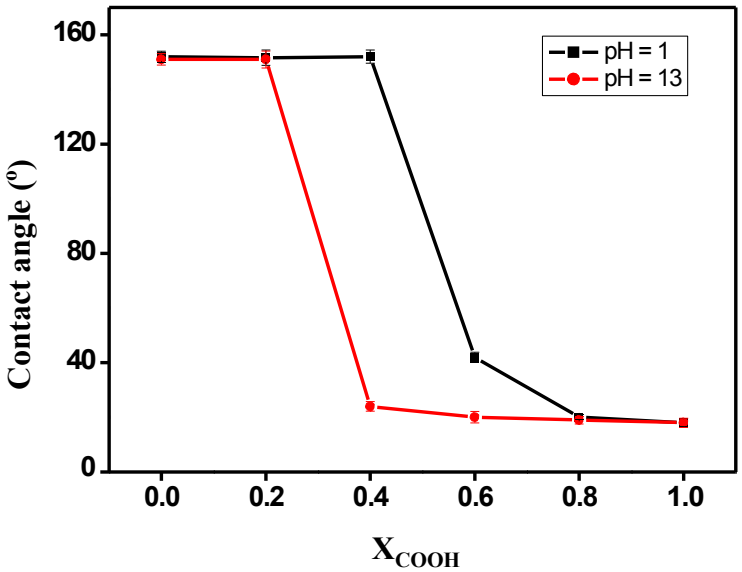

Fig. S14 Dependence of the water contact angle on the X_{COOH} (mole fraction of $HS(CH_2)_{10}COOH$ in the modified solution) for droplets with pH = 1 and 13 on the back surface (pH-responsive layer) of the pH-rJM.

From this figure, it can be seen that when the X_{COOH} = 0.4, the pH-responsive layer of the pH-rJM has the best controllability. The water contact angles can be changed from superhydrophobicity to high hydrophilicity as the water pH is varied from acid (pH = 1) to basic (pH = 13), which is similar as Yu's report.[3] Therefore, to obtain the best controllability, in this work, during the preparation process of pH-rJM, mixed thiol solution with X_{COOH} = 0.4 was used.

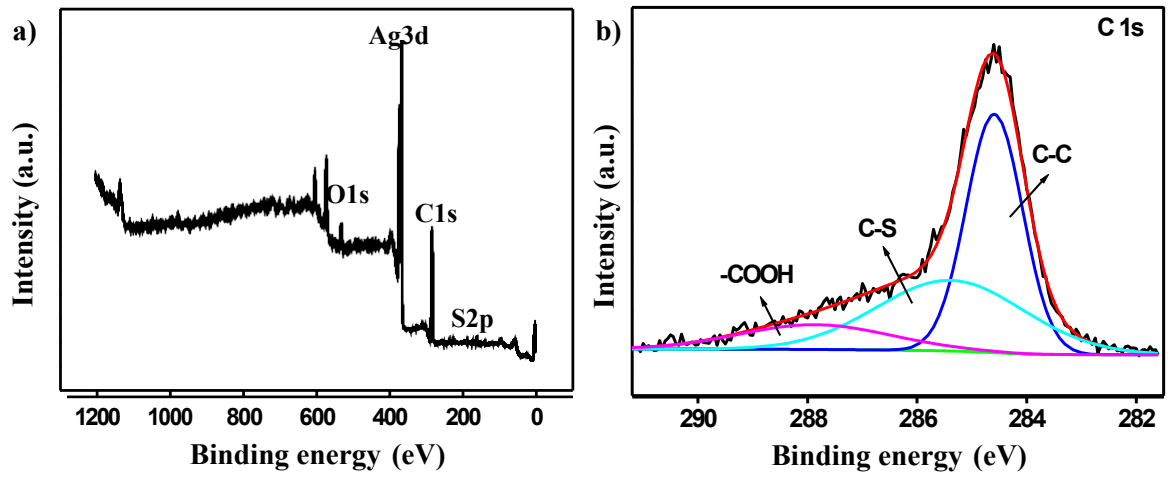

Fig. S15. (a) XPS survey spectrum of the flat Ag substrate modified with mixed thiol solution with X_{COOH} = 0.4 (X_{COOH} is defined as the mole fraction of $HS(CH_2)_{10}COOH$ in the modified solution); (b) high-resolution C1s spectra of the flat film.

From Fig. S15a, one can observe that element Ag, C, O, and S can be observed, means that thiol molecules have been assembled onto the flat Ag substrate. Fig. S15b shows the high-resolution C1s spectra, peaks ascribed to the methylene carbon, thiol carbon, and carboxyl carbon can be observed, respectively. Given every $HS(CH_2)_{10}COOH$ and $HS(CH_2)_9CH_3$ have

one C-S bonding, and every $HS(CH_2)_{10}COOH$ has one –COOH group, the peak area ratio between the -COOH and the C-S can be considered as the mole fraction of $HS(CH_2)_{10}COOH$ among total thiol molecules (all $HS(CH_2)_{10}COOH$ and $HS(CH_2)_9CH_3$ molecules) on the flat substrate (about 0.36 according to Fig. S15b), which is approximate to the X_{COOH} value (0.4) of the modified solution.

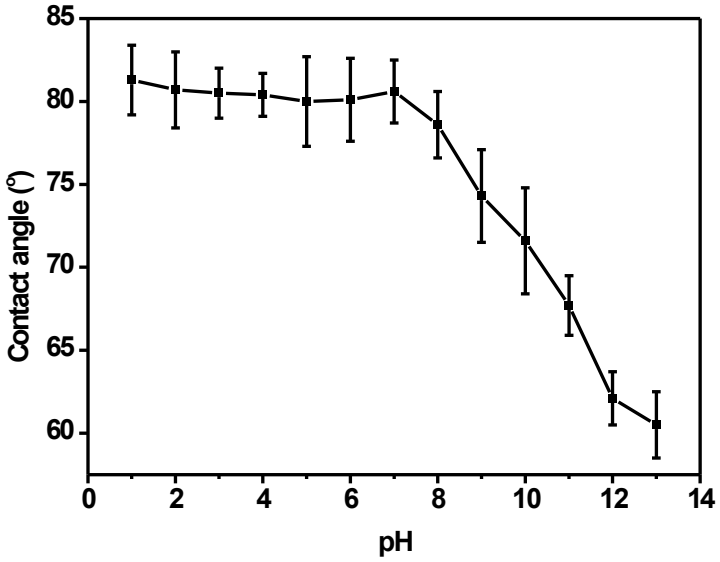

Fig. S16 The variation between the contact angles and water pH on flat substrate modified with $HS(CH_2)_9CH_3$ and $HS(CH_2)_{10}COOH$ with the similar ratio as that on the pH-rJM.

Discussion about pH-responsive wettability on the pH-rJM.

The pH-responsive wettting switch between superhydrophobicity and high hydrophilicity can be attributed to the following two factors: one is the variation of surface carboxylic acid groups between protonation and deprotonation as a function of aqueous pH,[3, 4] and the other is the rough structures on the substrates which can enhance the wetting performances.[5, 6] In this work, before modification with mixed thiol molecules, a Ag layer has been covered on the

membrane, which can react with the -SH groups, and the -COOH groups can be used as the functional groups.[3, 4] For nonalkaline water, the protonated carboxylic acid groups that show relative hydrophobicity present on the membrane (Scheme S2b). Together with the hydrophobic $HS(CH_2)_9CH_3$ and the amplified effect of surface rough structures, the superhydrophobicity and high contact angle can be observed on the obtained membrane, which can further be proved by the following equation:[5]

$$\cos\theta_r = f_1 \cos\theta - f_2 \quad (1)$$

Here, θ_r and θ are the water contact angles for a water droplet on the rough and flat substrates after modification with the same thiol molecules, respectively. f_1 and f_2 are the fraction of solid and air under the water droplet, respectively (i.e., $f_1 + f_2 = 1$). In this work, take water pH = 7 as an example, θ_r and θ are 152° (Fig. 5b) and 81° (Fig. S16), respectively. According to eq 1, $f_2 = 0.899$, indicating that the air fraction is enough high to induce the superhydrophobicity. Thus, for nonalkaline water, the water contact angles are higher than 150° (Fig. 5b). As the water pH is changed to the alkaline condition, the deprotonated carboxylic acid groups with better hydrophilicity are formed on the film (Scheme S2c, Fig. S16). Meanwhile, the hydrophilicity can be intensified by the rough structures according to the Wenzel equation.[6] As shown in Fig. S11, the presence of porous structure can effectively increase the surface roughness. Thus, water can enter into the rough structures for the three- dimensional capillary effect, and a low water contact angle and high hydrophilicity can be seen on the membrane.

3. Information of Movies

Video 1 Fabrication of JM via peeling off the top skin layer by adhesive tape.

Video 2 A water droplet penetrates through JM at the oil/water interface (the thin hydrophobic top surface towards oil).

Video 3 A water droplet is blocked by JM at the oil/water interface (the thick hydrophilic back surface towards oil).

Video 4 Capture and lossless transportation of water droplets via a collector fabricated by the JM (the thin hydrophobic surface of JM act as the outer surface of the collector).

Video 5 The MJM could be attracted by a magnet.

Video 6 A water droplet (containing 0.1M NaCl, pH=13) penetrates through pH-rJM at the oil/water interface (the hydrophobic surface towards oil), while other water droplets (containing 0.1M NaCl, pH=1 and pH=7, respectively) were blocked by the pH-rJM. (The top surface towards oil)

Video 7 A water droplet (pH=7, containing 1 mM $AgNO_3$) penetrates through pH-rJM (the peeled hydrophobic layer towards oil) when the water under the pH-rJM become alkaline with the adding of NaOH (The top surface towards oil).

Video 8 All water droplets with different pH value (pH=1, 7, 13, all containing 0.1M NaCl) were blocked when the pH-rJM was reversed (the back surface towards oil).

Video 9 A water droplet (pH=7, containing 1 mM $AgNO_3$) was still blocked by pH-rJM (the back surface towards oil) even the water under the pH-rJM become alkaline by adding NaOH.

4. References

1. H. Deng, X. Li, Q. Peng, X. Wang, J. Chen, Y. Li, *Angew. Chem. Int. Ed.,* 2005, **117**, 2842-2845.
2. B.H. Toby, *J. Appl. Crystallogr*., 2001, **34**, 210-213.
3. Y. Yu, Z. Wang, Y. Jiang, F. Shi, X. Zhang, *Adv. Mater*. 2005, **17**, 1289−1293.
4. C. D. Bain, G. M. Whitesides, *Langmuir* 1989, **5**, 1370−1378.
5. A. B. D. Cassie, S. Baxter, *Trans. Faraday Soc*. 1944, **40**, 546−551.
6. R. N. Wenzel, *Ind. Eng. Chem*. 1936, **28**, 988−994